DET NORSKE VIDENSKAPS-AKADEMI I OSLO

GEOFYSISKE PUBLIKASJONER
GEOPHYSICA NORVEGICA

Vol XXV. No. 3 February 1964

EIGIL HESSTVEDT

On the water vapor content in the high atmosphere

OSLO 1964
UNIVERSITETSFORLAGET

GEOFYSISKE PUBLIKASJONER
GEOPHYSICA NORVEGICA
VOL. XXV. NO. 3

ON THE WATER VAPOR CONTENT IN THE HIGH ATMOSPHERE

By Eigil Hesstvedt

FREMLAGT I VIDENSKAPS-AKADEMIETS MØTE DEN 6TE DESEMBER 1963 AV HØILAND

Summary. On the basis of a model for the general circulation in the stratosphere and mesosphere a possible explanation is presented for the observed increase with height from about 20 km of the water vapor mixing ratio. Upward motion through the tropical tropopause may be sufficiently strong to transport H_2O substance in the form of ice crystals into the stratosphere. This air mass will arrive in middle and high latitudes at heights of 25 km or more. — A combination of the proposed circulation model and a theoretical photochemical model atmosphere shows that the photodissociation of water vapor is unimportant below about 80 km. Above this height photodissociation causes a rapid decrease in the water vapor mixing ratio.

1. Introduction. Before measurements of the water vapor content in the stratosphere were made, it was generally assumed that the regions above the tropopause were very dry. This conclusion was based upon the absence of clouds above the tropopause (water or ice clouds were only rarely seen). The assumption of a dry lower stratosphere was later confirmed by frostpoint measurements up to about 15 km over England (Murgatroyd, Goldsmith and Hollings, 1955, Helliwell, Mackenzie and Kerley, 1957).

This peaceful state of affairs was brought to an end when direct measurements were extended to higher altitudes. Although large variations occur, these observations seem to indicate an increase in the mixing ratio by approximately an order of magnitude from 20 to 30 km (Gutnick, 1962). The phenomenon of an increasing mixing ratio with height has frequently been discussed in the literature, but so far, without being conclusively explained.

The water vapor content above the levels exposed to direct measurements has also attracted much interest, especially in connection with discussions on the problem of the nature of noctilucent clouds (Hesstvedt, 1962). In their study of the photochemistry of the oxygen-hydrogen atmosphere, Bates and Nicolet (1950) found that

the photodissociation of water vapor becomes significant as low as 65 km, thus excluding the possibility of ice cloud formation at the levels of noctilucent clouds.

It is the aim of this paper to discuss the two problems mentioned above. A possible explanation of the increase in mixing ratio from 20 to 30 km is given on the basis of circulation models for this part of the atmosphere. Furthermore, the general circulation is shown to raise the upper limit of the region of high water vapor content in the high latitude summer mesosphere to the levels where noctilucent clouds have been observed.

2. The general circulation in the stratosphere and the mesosphere. As already mentioned, the mixing ratio water vapor to air has been found to increase with height from about 15 km upwards to the limit of observations. The validity of the measurements has been questioned (GUTNICK, 1961), but no conclusive statement has so far been given. In this paper it will be assumed that the measurements are representative and that they give a realistic picture of the water vapor distribution in the region 15—30 km. As a consequence, the observed increase in mixing ratio with height requires an explanation.

The variations in water vapor content due to photochemical reactions are negligibly small. Water vapor will therefore act as a useful tracer and its spatial distribution will be closely related to the general circulation.

A theoretical study of the mean air flow between 15 and 80 km was recently made by MURGATROYD and SINGLETON (1961), who calculated vertical and meridional velocities for levels between 15 and 80 km, for all latitudes and for different periods of the year. In these calculations the eddy transport was neglected, a simplification which may have introduced considerable error into the final result. Further errors may have arisen from uncertainties in the data which were used as a basis for the determination of the rates of heating and cooling in the atmosphere. So far there is not enough observational data to serve as a check on MURGATROYD and SINGLETON's circulation models. In view of all the uncertainties involved, it is perhaps not advisable to draw too many and detailed conclusions about the water vapor circulation. Nevertheless it is of interest to use the models, and regard them as models only, to see if it is possible to reconcile the air flow in the model atmosphere with the observations of water vapor up to 30 km. In particular we want too see if it is possible to reconcile the stratospheric circulation, as determined by MURGATROYD and SINGLETON, and the observed increase in water vapor mixing ratio up to 30 km.

In order to obtain a better visual impression of the airflow in the upper atmosphere, the velocity vectors in the meridional plane were determined from the vertical and meridional velocities obtained from MURGATROYD and SINGLETON's figures. From the vector fields thus obtained, streamlines were drawn. MURGATROYD and SINGLETON divided the year into eight parts: early summer, mid-summer, late summer, autumn, early winter, mid-winter, late winter and spring. (Since symmetry was assumed between the two hemispheres, the results may be presented in four diagrams.) Thus each set of data may be said to represent a period of $1^1/_2$ months. The streamline patterns for

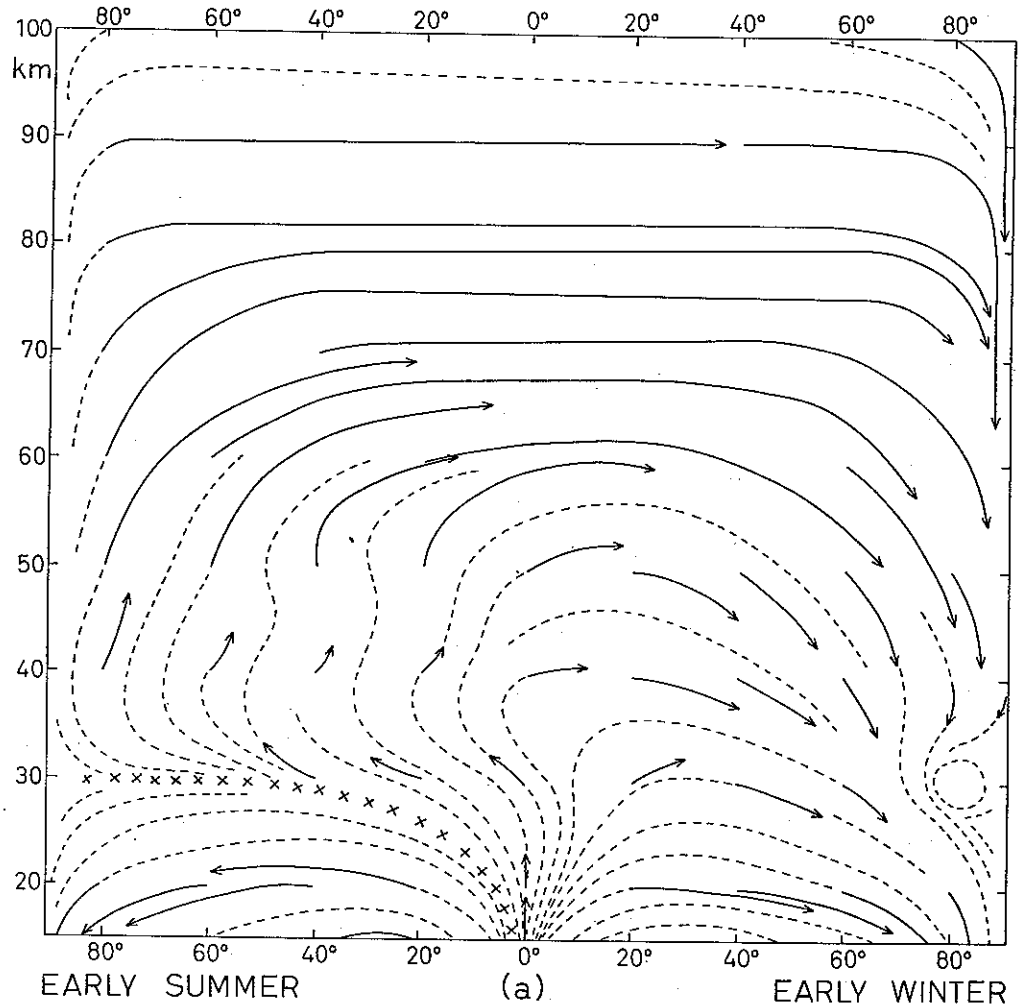

Fig. 1a. Mean motion in the upper atmosphere (based upon MURGATROYD and SINGLETON's data). The arrows indicate the distance travelled by air particles in 6 weeks (early summer and early winter).

the four periods early summer to autumn show marked similarities; a corresponding similarity also exists for the periods early winter to spring. Consequently the assumption of a stationary flow within a 45 day period does not seem to introduce significant errors in our computations. — Assuming stationary flow, we may compute the distance travelled by particles over a 45 day period. The results of such computations are shown in figure 1a—d. (In order to obtain a picture of the air flow just above the mesopause, MURGATROYD and SINGLETON's data were extended to 100 km by a "probable", but purely geometric, extrapolation. Obviously such a procedure introduces many uncertainties for the levels in question, but the errors are of minor importance for the evaluation of the water vapor content at high levels in section 4.)

A similar feature noted for all seasons is that the air enters the stratosphere in low latitudes, moves polewards in both hemispheres and reenters the troposphere in high

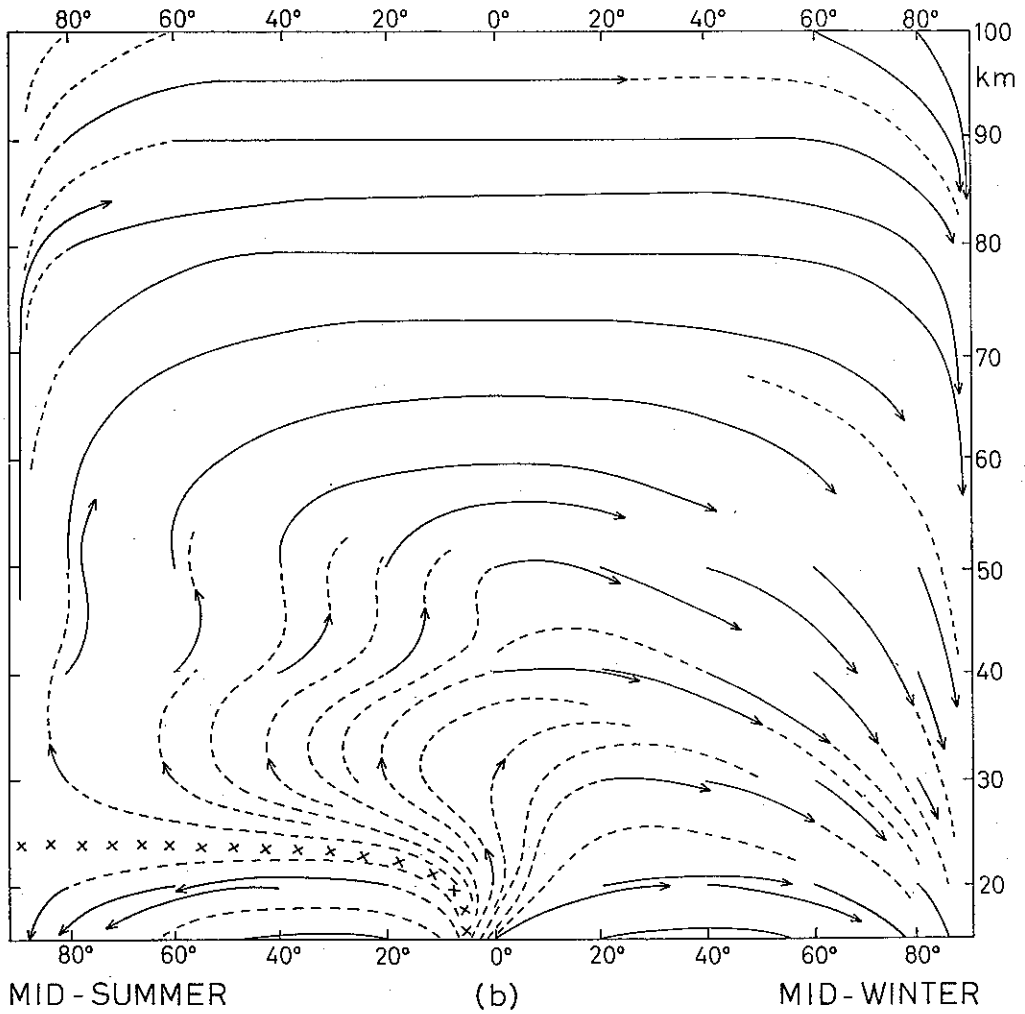

Fig. 1b. Same as fig. 1a for mid-summer and mid-winter.

latitudes. However during the summer season this poleward flow is seen to split up, one part going back to the troposphere and one part rising to higher parts of the stratosphere. The streamlines dividing these two flows, shown in the figures by crossed lines, are situated at a height of approximately 25 km. If we follow these lines back to the tropical tropopause, we find that the air entering the stratosphere on the poleward side of about 5—10° latitude never reaches altitudes higher than about 25 km, but sinks back to the troposphere in high latitudes.

In the same way we may show that air reaching the 30 km level in the winter hemisphere cannot have penetrated the tropical tropopause on the poleward side of 5° latitude.

Consequently the air masses at about 30 km or above can be traced back to a 10° latitude zone situated very close to the equator, drifting slightly north-south with the season. Therefore, if the water vapor content in this zone is significantly higher than

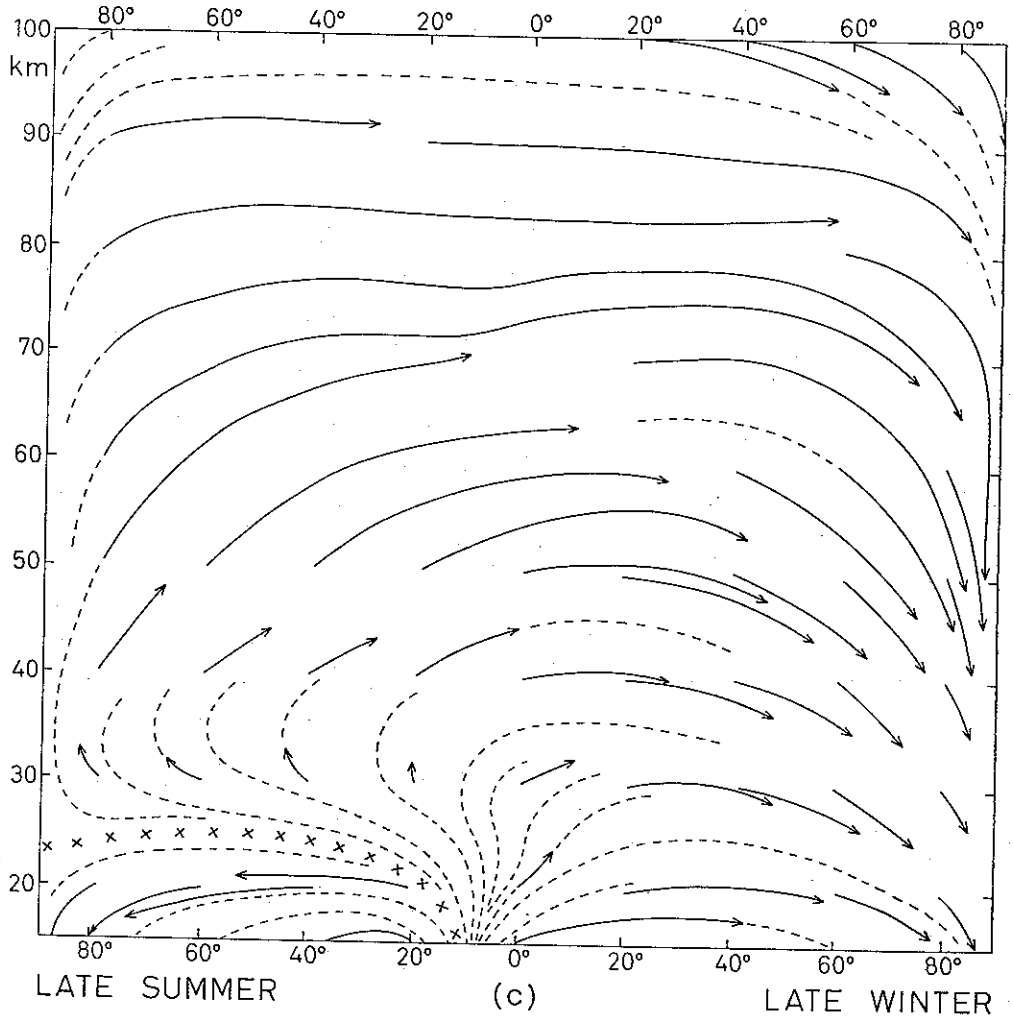

Fig. 1c. Same as fig. 1a for late summer and late winter.

that in the air in higher latitudes, one should expect the water vapor mixing ratio to increase with height in high and mid-latitudes.

The arguments in the discussion above rest upon a somewhat simplified picture of the air transport in the stratosphere. At certain levels this transport is very slow and the marked difference between the summer and winter circulation will give rather irregular curves for the trajectories in certain regions of our model atmosphere. However, it is difficult to see how the main features of the simplified picture of the circulation, as outlined above, could be seriously affected by integrations over longer periods of time.

3. The tropical tropopause as a source of high level humidity. It is generally accepted that the air rises in the tropical troposphere and enters the stratosphere either through the tropical tropopause or through the break in the tropopause in the tropical jet region. In both cases the air has to pass a region of extremely low

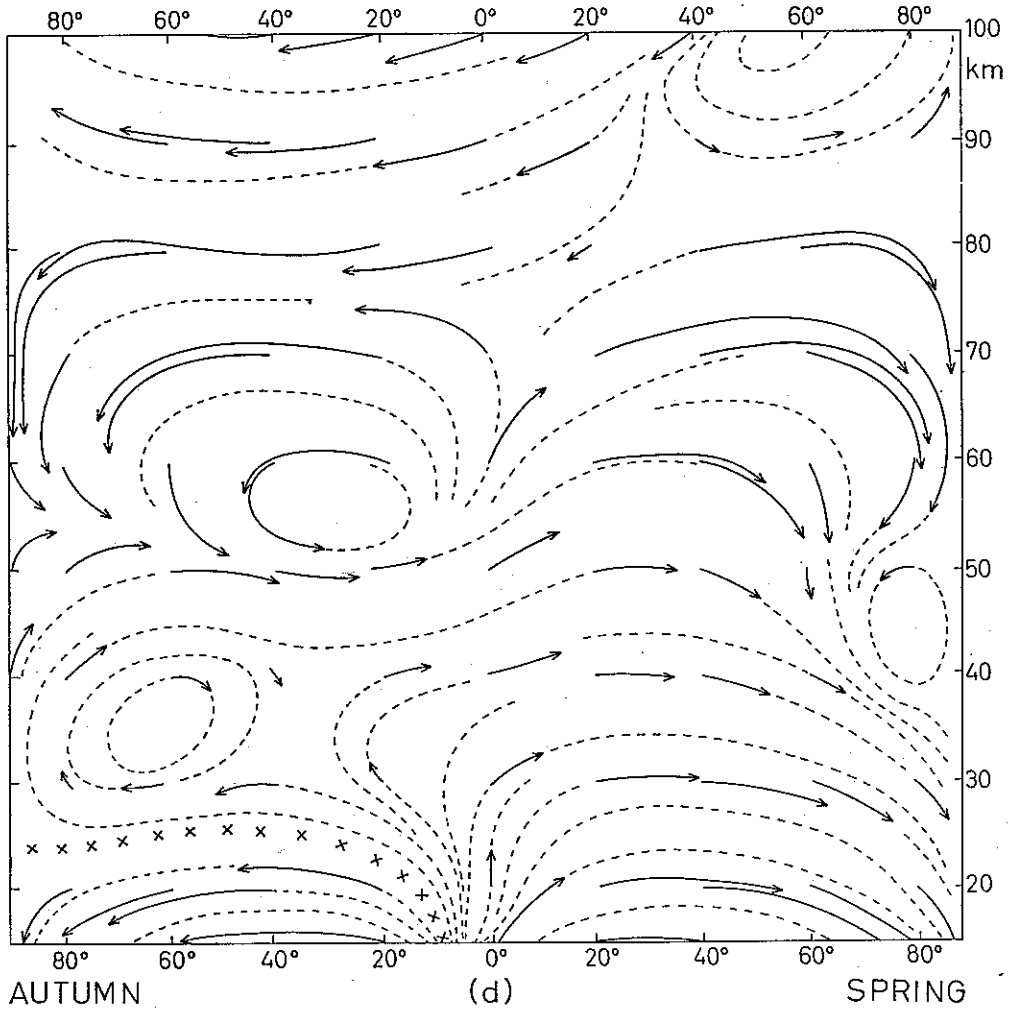

Fig. 1d. Same as fig. 1a for autumn and spring.

temperature, down to about −80°C. The excess of water vapor will then condense out and form ice crystals. If the fall velocity of these crystals is larger than the vertical velocity of the air they will fall down to lower levels. The temperature minimum will therefore act as a water vapor trap and ensure a constant humidity mixing ratio in the stratosphere, in agreement with the results of the frost-point observations made over the British Isles.

On the other hand, if the terminal fall velocity of the ice crystals is smaller than the upwind velocity the crystals will be carried by the air currents into the stratosphere, where they will evaporate at a certain level due to the increasing temperature.

This argument leads us to the following question: Is it possible that tiny ice particles are brought up within a narrow equatorial zone (width about 10°), as described in section 2, whereas the vertical velocities outside this zone are too small to prevent sedimentation of the ice crystals formed?

In order to give a tentative answer to this question, we shall compare the vertical

velocities in the equatorial zone with terminal fall velocities for particles of different sizes.

From MURGATROYD and SINGLETON's figures, 0.1 cm/sec seems to be a representative value for the vertical velocity of the air at about 18 km in the equatorial zone defined above. The movement in this zone is essentially vertical, the meridional component being negligibly small. Outside this zone the vertical velocities decrease very rapidly. In addition this effect is accelerated by the fact that the meridional transport soon brings the particles to latitudes where the vertical velocities are very small (and even change sign beyond 30° latitude).

Since the crystals will attain a prismatic rather than a spherical shape, a departure from Stokes' law must be expected. It is therefore necessary to determine the terminal fall velocity of different forms of hexagonal prisms. Due to small values of supersaturation only two crystal forms are likely to occur, namely columns and plates. We shall assume that multiple crystals do not occur. Furthermore the complex surface of a column will be approximated by an ellipsoid with semiaxes $[a, a, ka(k>1)]$, where $2a$ is the thickness of the crystal. In a similar way the hexagonal plate will be approximated by an ellipsoid with semiaxes $[b/k', b, b(k'>1)]$, where b is the mean radius of the hexagon. According to LAMB (1932), the resistence experienced by a falling ellipsoid is

$$6\pi\mu r v\,, \tag{3.1}$$

where μ = dynamic viscosity, v = fall velocity, and r = a characteristic length which depends upon

$$r = \frac{8}{3(I_1 + I_2 a^2)} \tag{3.2}$$

where

$$I_1 = \int_0^\infty \frac{d\lambda}{(a^2+\lambda)(k^2a^2+\lambda)^{1/2}}\,, \quad I_2 = \int_0^\infty \frac{d\lambda}{(a^2+\lambda)^2(k^2a^2+\lambda)^{1/2}} \tag{3.3}$$

which gives, upon integration

$$r = \frac{8a}{3}\,\frac{k^2-1}{k+(2k^2-3)(k^2-1)^{1/2}\ln(k+(k^2-1)^{1/2})} = a\cdot f(k) \tag{3.4}$$

For $2<k<10$ we may write $f(k)\approx 1+k/4$. — For a plate the expression for r becomes

$$r = \frac{8}{3(I_1' + I_2' b^2/k'^2)} \tag{3.5}$$

where

$$I_1' = \int_0^\infty \frac{d\lambda}{(b^2+\lambda)(b^2/k'^2+\lambda)^{1/2}}, \quad I_2' = \int_0^\infty \frac{d\lambda}{(b^2+\lambda)(b^2/k'^2+\lambda)^{3/2}} \tag{3.6}$$

which gives

$$r=\frac{4b}{3}\frac{k'^2-1}{k'+k'(k'^2-2)(k'^2-1)^{1/2}\left[\frac{\pi}{2}-\operatorname{arctg}(k'^2-1)^{-1/2}\right]}=b\cdot f'(k') \tag{3.7}$$

For $k'>2$ we may write $f'(k')\approx 0.85$.

From (3.1) and (3.4) the terminal fall velocity v_c of a column may be determined by assuming equilibrium between resistence and gravitational force:

$$v_c=\frac{2\rho_i g k a^2}{9\mu f(k)} \tag{3.8}$$

where ρ_i = density of ice and g = acceleration of gravity. — For the terminal fall velocity v_p of a plate we obtain:

$$v_p=\frac{2\rho_i g b^2}{9\mu k' f'(k')} \tag{3.9}$$

It is useful to compare the terminal fall velocity of a crystal to the terminal fall velocity v_s of a sphere of equal volume. The following relations are obtained

$$v_c=v_s\cdot\frac{k^{1/3}}{f(k)} \tag{3.10}$$

and

$$v_p=v_s\cdot\frac{1}{k'^{1/3}f'(k')}\,. \tag{3.11}$$

The values of the ratios v_c/v_s and v_p/v_s are shown in figure 2 for different values of k and k'. The ratios are smaller than unity, which means that single, compact ice crystals fall slower than an ice sphere of equal volume. However the difference is not so large that the assumption of a spherical crystal form is qualitatively misleading. We may therefore conclude that an updraft of 0.1 cm/sec near the tropopause, as determined by MURGATROYD and SINGLETON, is too small to prevent precipitation of medium and large cloud particles, but is sufficiently large to transport into the stratosphere small ice particles of "geometrical mean radius" about 3μ.

(Since the temperature rises above the tropopause, the small particles will start evaporating. This effect will compensate for the decrease with height of the vertical velocity.)

Standard values for the mixing ratio at heights up to 31 km have recently been given by GUTNICK (1962), who suggests $1.5\times 10^{-4} g/g$ as a representative value of the mixing ratio at 31 km, corresponding to a frostpoint temperature of $-70°$C at this level. If we trace this air mass back to its source region at lower levels in the tropics, all the time comparing with the air temperature field, we find that temperature and frostpoint are equal at about 22 km. Below 22 km supersaturation must exist, the major part of the excess of water vapor being taken up by ice particles. As we descend below

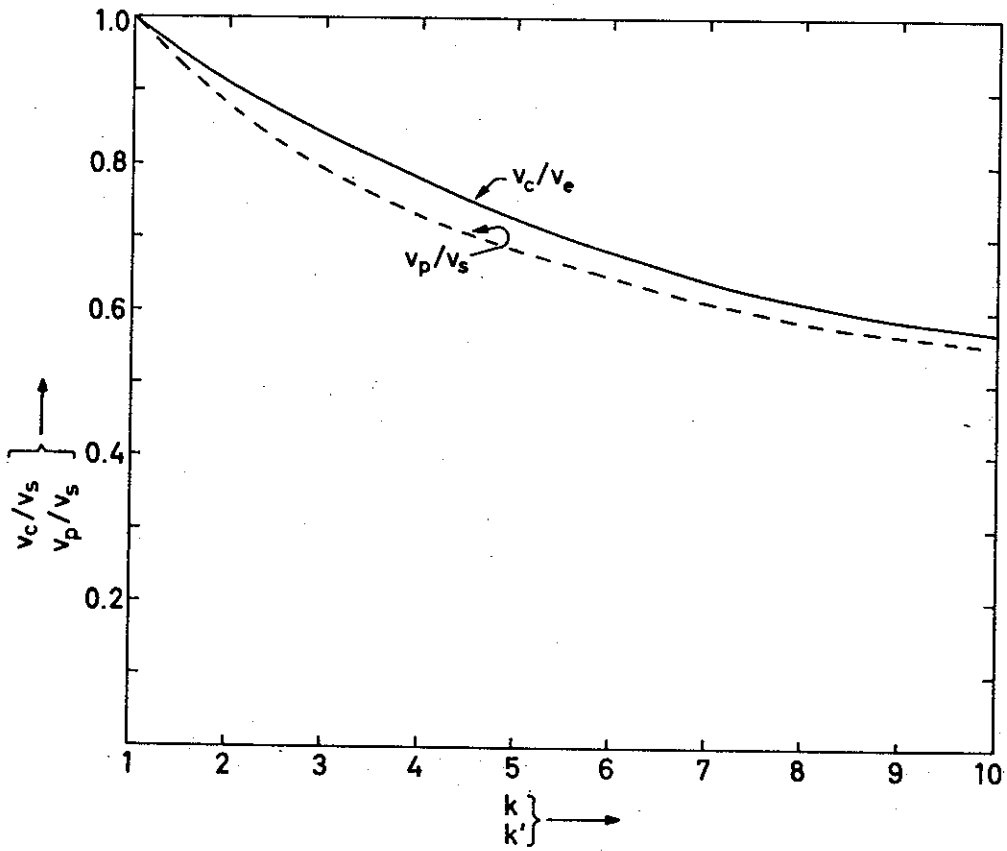

Fig. 2. The solid curve shows the ratio v_c/v_s of the terminal fall velocity v_c of an elongated ellipsoid of revolution, falling with the long axis horizontal, to the terminal fall velocity v_s of a sphere of equal volume (k=ratio of principal axes). The dashed curve shows the ratio v_p/v_s of the terminal fall velocity v_p of an oblate ellipsoid of revolution, falling with the short axis vertical, and the terminal fall velocity v_s of a sphere of equal volume (k'=ratio of principal axes). The two types of ellipsoids are assumed to be representative for columns and plate crystals.

18 km the temperature increases as we descend and temperature and frostpoint are again equal at a height of about 13 km. According to our hypothesis a continuous ice cloud should exist between 13 and 22 km, covering a belt of 10° latitude around the earth. We shall draw some further conclusions about this "hypotethical cloud".

From an evaluation of the actual total water content (given by the assumed mixing ratio and the vertical pressure profile) and the saturation vapor pressure with respect to ice (given by the temperature profile) we may compute the ice content at each level. The maximum value of the ice content was found to be 1.9×10^{-8}g/cm^3 at a height of 19 km. For a given vertical velocity we may compute the maximum volume of an ice crystal following the airflow upwards. Since the vertical velocity is quite small, the ice particles will have sufficient time to reach their equilibrium size. This makes it possible to estimate the concentration N of particles which is necessary to take up the required quantity of ice substance (1.9×10^{-8}g/cm^3). Figure 3 shows the results

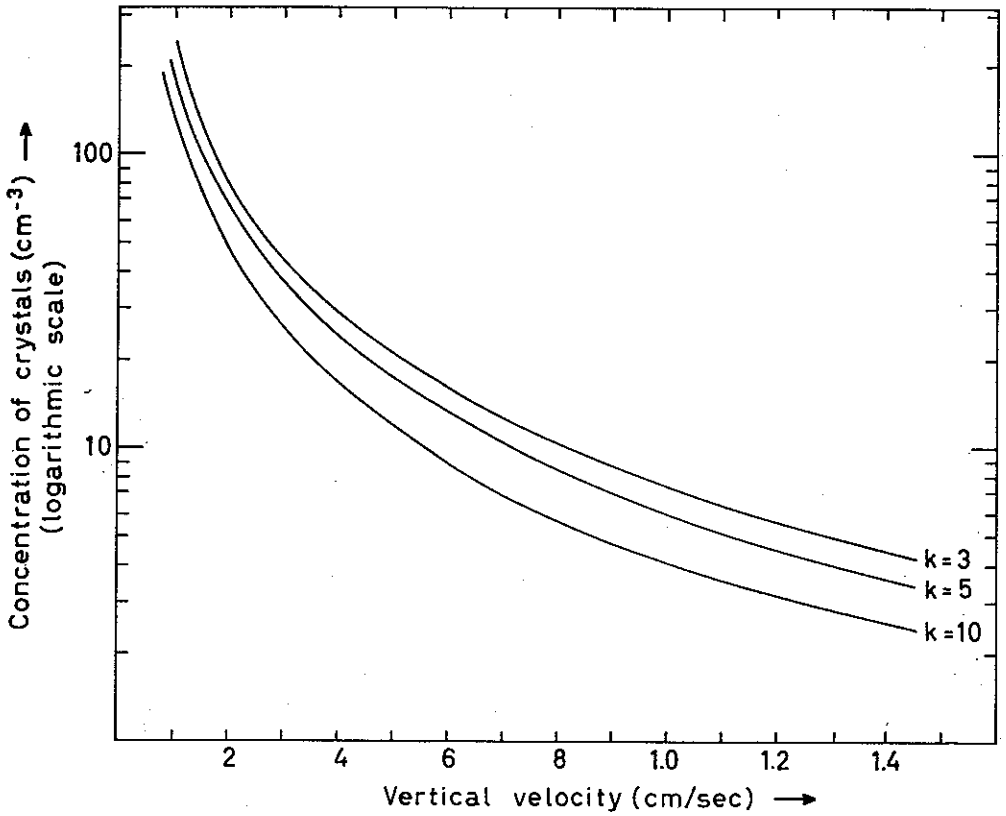

Fig. 3. The concentration (N) of ice crystals at the tropical tropopause required for a transport of water substance which is sufficient to explain the observed high mixing ratios above 25 km, plotted against vertical velocity.

of such computations for ice columns of length 3, 5 and 10 times the mean thickness. As might have been expected from the computations above the concentration N does not depend critically upon the crystal form. On the other hand N depends very strongly upon the vertical velocity. For a velocity of 0.1 cm/sec N must be larger than 100 cm^{-3}, whereas a velocity of 0.5 cm/sec reqpires only 10—20 particles pr. cm^3 Such clouds might be visible under favorable conditions (for instance viewed horizontally from an aircraft at about 18 km against a low sun). To the author's knowledge, there is no observational evidence of the existence of such a cloud. However it might be of interest to try to make samples of the atmospheric aerosol in the atmospheric region in question. If ice crystals were found here it could imply that the model which has been presented is a realistic one and could be used in future studies of the high altitude circulation and the mass exchange between troposphere and stratosphere.

4. The water vapor content above 30 km. We shall now turn to the second problem mentioned in section 1, a discussion of the humidity conditions at the levels above 30 km. Except for a single observation (PYBUS and YUNKER, 1962) no direct measurements are available, and our considerations will therefore be purely theoretical.

As already mentioned, a photochemical oxygen-hydrogen model atmosphere has been developed by BATES and NICOLET (1950). Since their paper was published our knowlegde of the temperature conditions in the upper atmosphere has improved considerably. Furthermore, additional radiation data are available and new values have been recommended for the rate coefficients of the recombination processes. It is therefore desirable to recompute the oxygen-hydrogen atmosphere model proposed by BATES and NICOLET.

In our oxygen-hydrogen atmosphere model we shall consider reactions between the following compounds: O, O_2, O_3, OH, HO_2, H_2, H_2O and H. In addition, non-reacting elements, M, will act as third bodies in three body collisions. Between these elements the following chemical reactions are considered:

(4.1)	$O+O+M\rightarrow O_2+M$	$k_1 = 1.6\times10^{-34}\cdot T^{1/2}\text{cm}^6\text{sec}^{-1}$
(4.2)	$O+O_2+M\rightarrow O_3+M$	$k_2 = 6.4\times10^{-36}\cdot T^{1/2}\text{cm}^6\text{sec}^{-1}$
(4.3)	$O+O_3\rightarrow 2O_2$	$k_3 = 4.2\times10^{-13}\cdot T^{1/2}e^{-3.2/RT}\text{cm}^3\text{sec}^{-1}$
(4.4)	$O_2+h\upsilon\rightarrow 2O$	$J_2 = 5\times10^{-7}\text{sec}^{-1}$ for zero optical depth
(4.5)	$O_3+h\upsilon\rightarrow O+O_2$	$J_3 = 10^{-2}\text{sec}^{-1}$ for zero optical depth
(4.6)	$H+O+M\rightarrow OH+M$	$k_6 = 6\times10^{-34}\cdot T^{1/2}\text{cm}^6\text{sec}^{-1}$
(4.7)	$H+O_2+M\rightarrow HO_2+M$	$k_7 = 1.3\times10^{-33}\cdot T^{1/2}\text{cm}^6\text{sec}^{-1}$
(4.8)	$H+O_3\rightarrow OH+O_2$	$k_8 = 8\times10^{-12}\cdot T^{1/2}e^{-1/RT}\text{cm}^3\text{sec}^{-1}$
(4.9)	$H+O_3\rightarrow HO_2+O$	$k_9 = 1.5\times10^{-11}\cdot T^{1/2}e^{-4/RT}\text{cm}^3\text{sec}^{-1}$
(4.10)	$OH+O\rightarrow H+O_2$	$k_{10} = 6.7\times10^{-12}\cdot T^{1/2}e^{-0.5/RT}\text{cm}^3\text{sec}^{-1}$
(4.11)	$HO_2+O\rightarrow OH+O_2$	$k_{11} = 6\times10^{-13}\cdot T^{1/2}\text{cm}^3\text{sec}^{-1}$
(4.12)	$HO_2+h\upsilon\rightarrow OH+O$	$J_{12} = 10^{-4}\text{sec}^{-1}$
(4.13)	$H_2O+h\upsilon\rightarrow OH+H$	$J_{13} = 1.5\times10^{-5}\text{sec}^{-1}$ for zero optical depth
(4.14)	$H+HO_2\rightarrow H_2O+O$	$k_{14} = 1.5\times10^{-11}\cdot T^{1/2}e^{-4/RT}\text{cm}^3\text{sec}^{-1}$
(4.15)	$H+HO_2\rightarrow H_2+O_2$	$k_{15} = 1.9\times10^{-13}\cdot T^{1/2}\text{cm}^3\text{sec}^{-1}$
(4.16)	$H+HO_2\rightarrow 2OH$	$k_{16} = 6\times10^{-13}\cdot T^{1/2}\text{cm}^3\text{sec}^{-1}$
(4.17)	$H+H+M\rightarrow H_2+M$	$k_{17} = 1.6\times10^{-33}\cdot T^{1/2}\text{cm}^6\text{sec}^{-1}$
(4.18)	$H+OH\rightarrow H_2+O$	$k_{18} = 1.5\times10^{-11}\cdot T^{1/2}e^{-4/RT}\text{cm}^3\text{sec}^{-1}$
(4.19)	$H_2+O\rightarrow OH+H$	$k_{19} = 4.5\times10^{-11}\cdot T^{1/2}e^{-7/RT}\text{cm}^3\text{sec}^{-1}$
(4.20)	$H_2+OH\rightarrow H_2O+H$	$k_{20} = 7\times10^{-12}\cdot T^{1/2}e^{-10/RT}\text{cm}^3\text{sec}^{-1}$
(4.21)	$OH+O_3\rightarrow HO_2+O_2$	$k_{21} = 1.5\times10^{-11}\cdot T^{1/2}e^{-4/RT}\text{cm}^3\text{sec}^{-1}$
(4.22)	$H+O_2\rightarrow OH+O$	$k_{22} = 3.6\times10^{-9}\cdot T^{1/2}e^{-24/RT}\text{cm}^3\text{sec}^{-1}$

(4.23) $OH+OH \rightarrow H_2O+O \qquad k_{23}=1.6\times10^{-13}\cdot T^{1/2}\text{cm}^3\text{sec}^{-1}$

(4.24) $OH+HO_2 \rightarrow H_2O+O_2 \qquad k_{24}=6\times10^{-13}\cdot T^{1/2}\text{cm}^3\text{sec}^{-1}$

Here $k_1, k_2, \ldots k_{24}$ are the rate coefficients for the recombination processes, and J_2, J_3, J_{12} and J_{13} are dissociation rates. The time variations of the eight components are given by eight differential equations:

(4.25) $$\frac{d[O]}{dt}=A_1-B_1[O]-C_1[O]^2$$

(4.26) $$\frac{d[O_2]}{dt}=A_2-B_2[O_2]$$

(4.27) $$\frac{d[O_3]}{dt}=A_3-B_3[O_3]$$

(4.28) $$\frac{d[OH]}{dt}=A_4-B_4[OH]-C_4[OH]^2$$

(4.29) $$\frac{d[HO_2]}{dt}=A_5-B_5[HO_2]$$

(4.30) $$\frac{d[H_2]}{dt}=A_6-B_6[H_2]$$

(4.31) $$\frac{d[H_2O]}{dt}=A_7-B_7[H_2O]=A_7-J_{13}[H_2O]$$

(4.32) $$\frac{d[H]}{dt}=A_8-B_8[H]-C_8[H]^2$$

Brackets [ ] are used to denote the particle concentrations of the components. In the equations (4.25) to (4.32) are also included the relations

(4.33) $$[O_2]+[HO_2]+\frac{1}{2}([O]+3[O_3]+[OH]+[H_2O])=\alpha[M]$$

(4.34) $$[H_2]+[H_2O]+\frac{1}{2}([OH]+[HO_2]+[H])=\beta[M]$$

expressing that the total amounts of oxygen and hydrogen at a given level are constant. For α we take the usual value 0.2095. Since practically all atmospheric hydrogen is

in the form of H_2O below about 70 km we shall assume the value $\beta = 2.4 \times 10^{-4}$ observed at 31 km. (The escape of high level hydrogen is neglected since it is unimportant below 100 km, which is the part of the atmosphere we want to examine in more detail.)

Since all the rate coefficients $k_1, k_2, \ldots k_{24}$ depend upon the temperature, and since [M] is a function of temperature and pressure, we have to specify a temperature and pressure profile for our model atmosphere. Due to seasonal and latitudinal temperature variations, which are especially pronounced near the mesopause, it is necessary to select at least three different profiles. NORDBERG and STROUD (1961) have computed mean temperatures for low latitudes (year) and for high latitudes (winter and summer separately). Their profiles were, with a slight revision, selected for the present calculations. (See table 1.)

Table 1. *Assumed temperature profiles for low latitudes and high latitudes, summer and winter.*

Height, km	Low latitude, summer and winter	High latitude, summer	High latitude, winter
120	350°K	350°K	350°K
110	257	257	270
100	236	232	256
100	218	212	242
95	203	196	231
90	190	178	223
85	185	161	217
80	190	163	215
75	200	188	219
70	219	212	225
60	247	254	252
50	270	274	259
40	254	254	230
30	233	234	200

The dissociation rates J_2 and J_3 were determined from the diagrams of DÜTSCH (1956) and NICOLET (1958). The dissociation rates are functions of the total amount of O_2 and O_3 in the overlying part of the atmosphere in the path of the sun's rays. Therefore, the sun's elevation also has to be taken into account. In low latitudes, the sun was assumed to be in zenith during daytime. For high (60°) latitude, mid-summer, the mean elevation during daytime was assumed to be 30°, and for high latitude, mid-winter, the mean elevation during the day was taken as 4.5°.

The dissociation rate for H_2O was calculated for the Lyα region and for the continuum 1500—1900 Å. The Lyα radiation was found to contribute significantly to the dissociation rate down to 60 km in low latitudes, down to 65 km in the high latitudes summer and down to 75 km in the high latitudes winter. It was found that for zero

optical depth one third (5×10^{-6}sec^{-1}) of the total dissociation rate was due to Lyα radiation.

Daytime equilibrium values may now be computed for our three model atmospheres by assuming the time variations in equations (4.25) to (4.32) to be zero. The resulting system of eight equations, in a suitable way combined with (4.33) and (4.34), was solved by an iterative method for each level and for the three atmospheric models.

The solutions thus obtained represent the equilibrium concentrations in a static atmosphere during an infinitely long day. No account has so far been taken to the effect of the interruptions in solar radiation during the night. Strictly the time variations of the concentrations should be found by integrations over 24 hour periods. However, sufficiently good approximations for the daytime concentrations are obtained if all the dissociation rates are multiplied by the ratio $t_d/24$ where t_d = length of the day in hours. The results of these computations are shown in figure 4, where the mixing ratio water vapor concentrations/total particle concentration is plotted against height. It is seen that all atmospheric hydrogen is in the form of H_2O up to a height of 70 km (75 km in the high latitude winter atmosphere) where dissociation causes an abrupt decrease in the water vapor mixing ratio by approximately one order of magnitude per 3 km. For instance, at 82 km in the high latitude summer atmosphere the mixing ratio is four orders of magnitude lower than at 70 km. This means that the frost point drops from 174°K at 70 km to 126°K at 82 km in our model atmosphere. A formation of ice clouds is not very likely under such conditions.

It should be mentioned that a diurnal variation in the water vapor content will occur due to the absence of solar radiation during the night. Below 80 km the nocturnal increase in the water vapor concentration is negligibly small. Between 80 km and 100 km the difference between the morning maximum and the evening minimum amounts to about 10% of the total concentration. At still higher levels this difference increases to about 30% in relative measure, but here the concentrations are so small that the problem is of academic interest only. Consequently, the simplified procedure chosen for the calculations in this section will hardly effect the results significantly.

The variations with height of the water vapor mixing ratio, shown in figure 4, are based upon the assumption of a static atmosphere. We shall next estimate the effect of the large scale motions upon the water vapor content in the mesopause region. It is clear that if the air rises, the mixing ratio at a given height will be higher than the equilibrium values shown in figure 4. Conversely, in descending air masses the mixing ratios will be lower than the equilibrium values. The magnitude of this effect will depend upon the vertical wind velocity and the characteristic time for the photodissociation of water vapor. An estimate of the latter effect can be made as follows: If the photochemical equilibrium in a static atmosphere is disturbed, the restoration of equilibrium may be found from integration of (4.31).

The quantity A_7 occurring in (4.31) consists of four terms, of which the term $k_{14}[HO_2] \cdot [H]$, corresponding to reaction (4.14) is dominating. The calculations show that the characteristic time for $[HO_2]$ is very small at all levels. Therefore $[HO_2]$

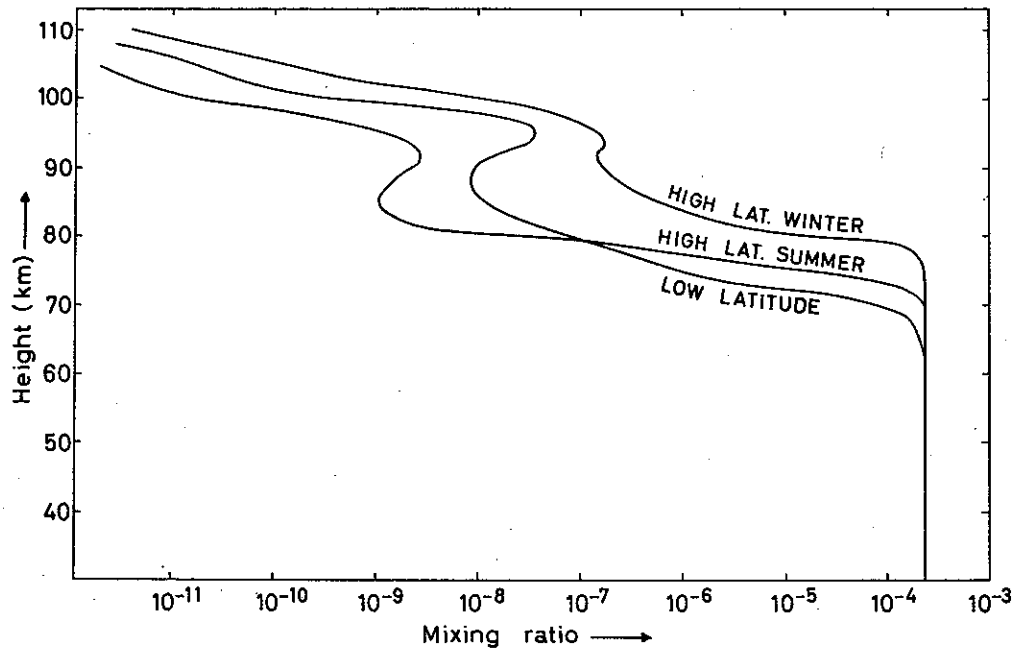

Fig. 4. Mixing ratios water vapor/air in a static atmosphere.

will always attain a kind of equilibrium value, determined by the current concentrations of the other components. As for H, its characteristic time is very short at low levels, gradually increasing to large values at high levels. At 85 km it is about 2—3 hours and at 90 km it has increased to 10—20 hours. If these times are compared to the motions described in figure 1a—d, we may conclude that [H] will always attain an equilibrium value, determined by the current concentrations of the other components, at all levels up to about 100 km. With an accuracy which is sufficient for our calculations we may assume that, during the motion of the air, A_7 will always have the value corresponding to photochemical equilibrium. Accordingly, the time variation of $[H_2O]$ will approximately be given by

$$[H_2O] = [H_2O]_e + ([H_2O]_0 - [H_2O]_e)\exp(-J_{13}t) \tag{4.35}$$

where $[H_2O]_o$ is the concentration of H_2O at $t=0$ and $[H_2O]_e$ is the concentration at $t=\infty$ (i.e. the equilibrium value). The characteristic time for restoration of photochemical equilibrium of H_2O is then $\tau = 1/J_{13}$. The variation of τ with height is shown in figure 5. At high levels (above 105 km) τ is about 20 hours. Below 105 km τ increases to large values. At 80 km in the high latitude summer, the characteristic time is seen to be about 5 days. Comparison of figure 1 and figure 5 shows qualitatively that upward notion is only likely to affect the water vapor mixing ratio at levels between 70 km and somewhat below 100 km.

Of special interest to our problem is the effect of the air motion upon the water vapor content in the high latitude summer atmosphere. In order to try to find how far

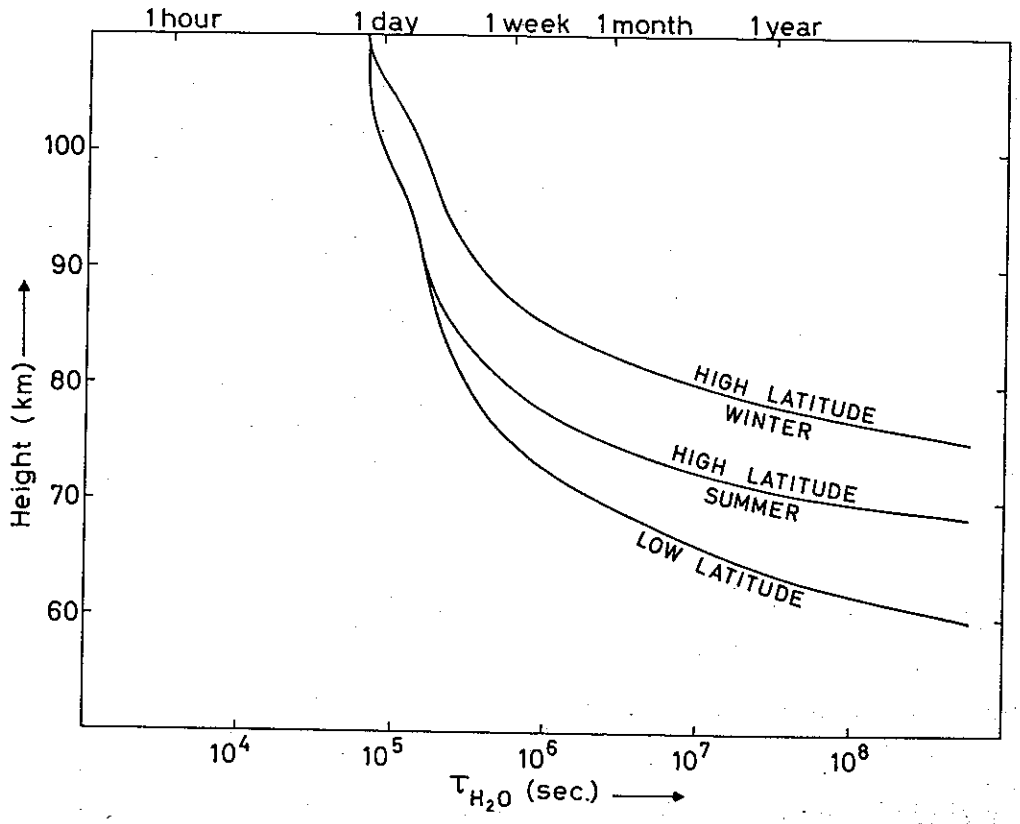

Fig. 5. Characteristic time (defined as $1/J_{13}$) for restoration of photochemical equilibrium of water vapor.

the dissociation level is raised above 70 km, which is the level of dissociation in a static atmosphere, we shall use equation (4.35) and select trajectories and vertical velocities in accordance with figure 1b. The water vapor mixing ratios computed in this way for the high latitude summer atmosphere are shown in figure 6. It is seen that the motion in our model will raise the level where photodissociation of water vapor becomes important by about 5 km, from 70 km to about 75 km during the summer in high latitudes. Above 75 km the photodissociation causes a rapid decrease in the water vapor mixing ratio. At 83 km the mixing ratio is one order of magnitude lower than it is at 75 km.

As for the water vapor content in low latitudes and in high latitudes in the winter hemisphere it is important to note that according to our circulation models the motion is essentially horizontal from 60° latitude in the summer hemisphere towards the equator and the winter hemisphere. The variation in the water vapor content due to the meridional transport can be computed from (4.35). Such computations have been made for 30° (summer hemisphere), equator, 30° (winter hemisphere) and 60° (winter hemisphere). The results are given in figure 6. It is seen that the water vapor content graddually decreases during the transport from 60° in the summer hemisphere to 30° in the winter hemisphere, but the values are at all times significantly higher than the

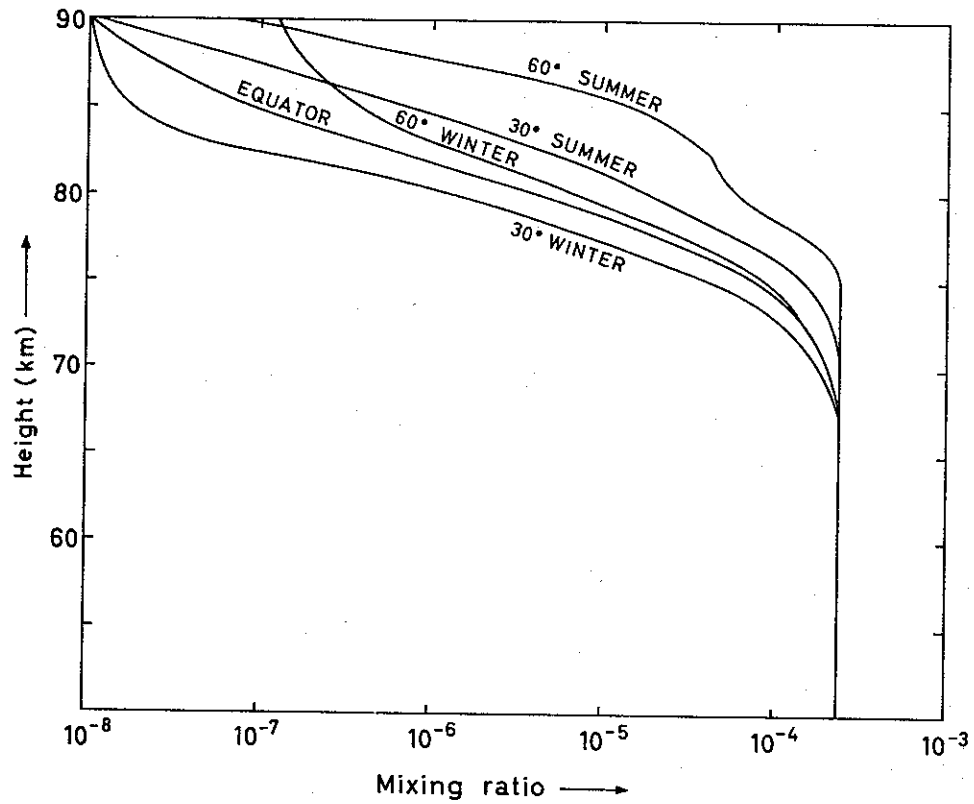

Fig. 6. Mixing ratios water vapor/air in an atmosphere with motion in accordance with figure 1 a—d.

equilibrium values shown in figure 4. During the transport from 30° to 60° in the winter hemisphere the mixing ratio increases again, but will be lower than the equilibrium value when it arrives at 60° latitude. On its trajectory towards the winter pole the air starts descending at a rate which will have a significant effect upon the mixing ratio. It is of interest to note that the static atmosphere model showed the highest content of water vapor at the mesopause level to occur near the winter pole. However, the air motion reverses this picture so that this region provides a drier mesopause than all other latitudes.

Now the following question arises: Is it possible to reconcile the results above with the assumption that noctilucent clouds consist of ice particles (HESSTVEDT, 1962)? Such clouds occur at about 82 km in high latitudes during the summer where the lowest temperatures of the entire atmosphere are found. If the water vapor mixing ratio were the same throughout the atmosphere the maximum possibility of supersaturation to exist should occur just at the high latitude summer mesopause. However, photodissociation will cut off the even distribution of water vapor at a height of about 75 km, according to our results. Still the mixing ratio calculated for 82 km (5×10^{-5}g/g corresponding to a frostpoint of 159°K) is high enough to explain supersaturation and

formation of ice particles. On the other hand this mixing ratio is possibly too low to explain relatively rapid variations in particle size (HESSTVEDT, 1962). But in view of all the uncertainties involved in the calculations the discrepancy is not such that ice particle formation and growth may be considered as unlikely.

5. Concluding remarks. Our knowledge about the circulation in the stratosphere and the mesosphere is at the present rather incomplete. It is shown above that a more detailed knowledge is necessary to explain some characteristics of the spatial distribution of water vapor in the high atmosphere. Extended studies on high level atmospheric circulation is therefore highly desirable. On the other hand more extensive observations of stratospheric humidity could possibly provide a clue to the understanding of the circulation in the lower stratosphere.

REFERENCES

BATES, D. R., and M. NICOLET, 1950: The photochemistry of atmospheric water vapor. *J. Geophys. Res.*, **55**, pp. 301—327.

DÜTSCH, H. U., 1956: Atmosphärisches Ozon als Indikator für Strömungen in der Stratosphäre. *Arch. Meteor., Geophys. und Biokl.*, **9**, pp. 87—119.

GUTNICK, M., 1961: How dry is the sky? *J. Geophys. Res.*, **66**, pp. 2867—2871.

— 1962: Mean annual mid-latitude moisture profiles to 31 km. *Air Force Surveys in Geophysics*, No. 147, July 1962.

HELLIWELL, N. C., J. K. MACKENZIE and M. E. KERLEY, 1957: Some further observations from aircraft of frostpoint and temperature up to 50,000 feet. *Quart. J. R. Meteor. Soc.*, **83**, pp. 257—262.

HESSTVEDT, E. 1962: On the possibility of ice cloud formation at the mesopause. *Tellus*, **14**, pp. 290—296.

LAMB, H., 1932: *Hydrodynamics*. (Dover Publications, New York).

MURGATROYD, R. P., P. GOLDSMITH, and W. E. H. HOLLINGS, 1955: Some recent measurements of humidity from aircraft up to heights of about 50,000 feet over Southern England. *Quart. J. R. Meteor. Soc.* **81**, pp. 533—537.

MURGATROYD, R. P., and F. SINGLETON, 1961: Possible meridional circulations in the stratosphere and mesosphere. *Quart. J. R. Meteor. Soc.*, **87**, pp. 125—135.

NICOLET, M., 1958: Aeronomic conditions in the mesosphere and lower thermosphere. *Ionospheric Research*, Scientific Report No. 102, Pennsylvania State University.

NORDBERG, W., and W. G. STROUD, 1961: Results of IGY rocket-grenade experiments to measure temperature and winds above the Island of Guam. *J. Geophys. Res.*, **66**, pp. 455—464.

PYBUS, E., and P. YUNKER, 1962: An unusually high altitude water vapor profile. (Paper presented at the spring 1962 meeting of the American Geophysical Union.)

Avhandlinger som ønskes opptatt i «Geofysiske Publikasjoner», må fremlegges i Videnskaps-Akademiet av et sakkyndig medlem.

Vol. XXI.

No. 1. A. Omholt: Studies on the excitation of aurora borealis II. The forbidden oxygen lines. 1959.
» 2. Tor Hagfors: Investigation of the scattering of radio waves at metric wavelengths in the lower ionosphere. 1959.
» 3. Håkon Mosby: Deep water in the Norwegian Sea. 1959.
» 4. Søren H. H. Larsen: On the scattering of ultraviolet solar radiation in the atmosphere with the ozone absorption considered. 1959.
» 5. Søren H. H. Larsen: Measurements of atmospheric ozone at Spitsbergen (78°N) and Tromsø (70°N) during the winter season. 1959.
» 6. Enok Palm and Arne Foldvik: Contribution to the theory of two-dimensional mountain waves 1960.
» 7. Kaare Pedersen and Marius Todsen: Some measurements of the micro-structure of fog and stratus-clouds in the Oslo area. 1960.
» 8. Kaare Pedersen: An experiment in numerical prediction of the 500 mb wind field. 1960.
» 9. Eigil Hesstvedt: On the physics of mother of pearl clouds. 1960.

Vol. XXII.

No. 1. L. Harang and K. Malmjord: Drift measurements of the E-lager at Kjeller and Tromsø during the international geophysical year 1957—58. 1960.
» 2. Leiv Harang and Anders Omholt: Luminosity curves of high aurorae. 1960.
» 3. Arnt Eliassen and Enok Palm: On the transfer of energy in stationary mountain waves. 1961.
» 4. Yngvar Gotaas: Mother of pearl clouds over Southern Norway, February 21, 1959. 1961.
» 5. H. Økland: An experiment in numeral integration of the barotropic equation by a quasi-Lagrangian method. 1962.
» 6. L. Vegard: Auroral investigations during the winter seasons 1957/58—1959/60 and their bearing on solar terrestrial relationships. 1961.
» 7. Gunnvald Bøyum: A study of evaporation and heat exchange between the sea surface and the atmosphere. 1962.

Vol. XXIII.

No. 1. Bernt Mæhlum: The sporadic E auroral zone. 1962.
» 2. Bernt Mæhlum: Small scale structure and drift in the sporadic E layer as observed in the auroral zone. 1962.
» 3. L. Harang and K. Malmjord: Determination of drift movements of the ionosphere at high latitudes from radio star scintillations. 1962.
» 4. Eyvind Riis: The stability of Couette-flow in non-stratified and stratified viscous fluids. 1962.
» 5. E. Frogner: Temperature changes on a large scale in the arctic winter stratosphere and their probable effects on the tropospheric circulation. 1962.
» 6. Odd H. Sælen: Studies in the Norwegian Atlantic Current. Part II: Investigations during the years 1954—59 in an area west of Stad. 1963.

Vol. XXIV.

In memory of Vilhem Bjerknes on the 100th anniversary of his birth. 1962.

Vol. XXV.

No. 1. Kaare Pedersen: On quantitative precipitation forecasting with a quasi-geostrophic model. 1963.
» 2. Peter Thrane: Perturbations in a baroclinic model atmosphere. 1963.

A.s John Griegs Boktrykkeri